

# Class H cement hydration at 180 °C and high pressure in the presence of added silica

Andrew C. Jupe<sup>a</sup>, Angus P. Wilkinson<sup>a,\*</sup>, Karen Luke<sup>b</sup>, Gary P. Funkhouser<sup>c</sup>

<sup>a</sup> School of Chemistry and Biochemistry, Georgia Institute of Technology, Atlanta, GA 30332-0400, USA

<sup>b</sup> Formerly with Halliburton, now with Trican Well Services Ltd. R&D Centre, 11979-40th Street S.E., Calgary, AB T2Z 4M3, Canada

<sup>c</sup> Halliburton, Duncan Technology Center, 2600 South 2nd Street, Duncan, OK 73536-0470, USA

Received 13 December 2006; accepted 17 December 2007

## Abstract

Under deep oil-well conditions of elevated temperature and pressure, crystalline calcium silicate hydrates are formed during Portland cement hydration. The use of silica rich mineral additives leads to the formation of crystalline hydrates with better mechanical properties than those formed without the additive. The effects of silica flour, silica fume (amorphous silica), and a natural zeolite mixture on the hydration of Class H cement slurries at 180 °C under externally applied pressures of 7 and 52 MPa are examined in real time using *in-situ* synchrotron X-ray diffraction. For some compositions examined, but not all, pressure was found to have a large effect on the kinetics of crystalline hydrate formation. The use of silica fume delayed both C<sub>3</sub>S hydration and the formation of crystalline silicate hydrates compared to what was seen with other silica sources.

© 2007 Elsevier Ltd. All rights reserved.

**Keywords:** Hydration; X-ray diffraction; Silica fume; Oil well cement

## 1. Introduction

The early hydration of oil-well cements is of considerable practical significance, as the cement slurry must be pumpable until the cement is in place, and the rapid development of mechanical strength soon after placement is needed to prevent both gas ingress and time lost waiting on the cement. The set-accelerating effects of elevated temperature are controlled by the addition of retarders. However, elevated temperature also leads to the formation of high calcium-to-silicon ratio crystalline silicate hydrates such as C<sub>3</sub>SH<sub>1.5</sub> (C<sub>3</sub>S hydrate or Jaffeite) and C<sub>2</sub>SH ( $\alpha$ -C<sub>2</sub>S hydrate), rather than C–S–H gel, which are deleterious to the mechanical properties of the resulting slurry [1]. The slurry properties can be improved by the use of silica-rich additives so that other crystalline hydrates are formed. Provided that sufficient siliceous material is added to bring the C/S ratio down to 1.0 or lower, the main hydration product at

180 °C will normally be tobermorite [2] which gives good compressive strength [3,4]. Portlandite is consumed during the production of tobermorite, and its absence from the resulting cement slurry is potentially advantageous in chemically-aggressive environments [5].

At high temperatures (>150 °C) the conversion of tobermorite to xonotlite, with an associated volume reduction, can occur. This volume reduction can be prevented by Al substitution [3,6,7]. Chemical analysis indicates that aluminum substitutes predominantly for silicon [8]. NMR measurements [9] indicate that there is no substitution of aluminum on calcium sites, suggesting the substitution of OH<sup>-</sup> for O<sup>2-</sup> to maintain charge balance. The incorporation of aluminum into C–S–H gel is thought to occur in a similar fashion [10]. The maximum extent of aluminum substitution in tobermorite is ~20% [11]. The incorporation of other elements, such as Fe and Mg, into tobermorite has been shown to be possible, but more difficult [12], and it does not seem to be an important issue in cement chemistry. Aluminum substitution up to 8% apparently enhances the compressive strength of tobermorite [6].

\* Corresponding author. Tel.: +1 404 894 4036; fax: +1 404 894 7452.

E-mail address: [angus.wilkinson@chemistry.gatech.edu](mailto:angus.wilkinson@chemistry.gatech.edu) (A.P. Wilkinson).

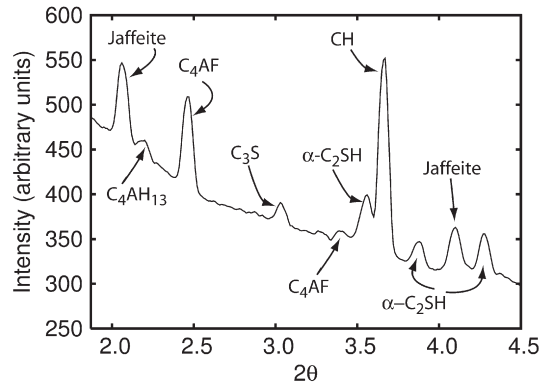


Fig. 1. Example powder diffraction data for the Class H control (Slurry 1) 100 min into its hydration.

There have been several studies of how aluminum substitution modifies the unit cell dimensions of tobermorite, with diverse results. The (002)  $d$ -spacings for pure and 10% Al-substituted tobermorite have been reported as 11.20 and 11.35 Å [12]; 11.4 and 11.6 Å [13]; and 11.31 and 11.44 Å [11] respectively. In all cases, the aluminum content was defined as the mole ratio Al/(Al+Si). A range of 11.1 to 11.7 Å has also been reported [8], but without precise estimates of the samples' aluminum contents. Even though there is considerable variation in the reported absolute values, the available data indicate that  $d_{(002)}$  increases with greater aluminum substitution. The crystallization of tobermorite is said to be accelerated by 1% or more Al substitution [8].

Cement slurries can be subject to significant hydrostatic pressure. Although studies of hydration reactions under pressure have been performed [4,14], very little published work explicitly examines the effects of pressure on reaction kinetics. The accelerating effect of 500 bar pressure on  $C_3S$  hydration has been demonstrated [15], and in an early study [16] the hydration of an OPC (measured by thermogravimetry) was found to be accelerated under 75 MPa hydrostatic pressure. The later work reported that the release of pressure led to still further acceleration of the hydration process, emphasizing the importance of *in-situ* measurements.

The current work examines the use of silica flour, silica fume (an amorphous silica by-product of ferrosilicon or silicon production), and a mixed natural zeolite, as additives in cement slurries hydrated at 180 °C and pressures of ~7 and 52 MPa using *in-situ* diffraction methods. The upper pressure of 52 MPa was dictated by the design of the pressure cell and the lower was chosen as a point of comparison suitable for use at 180 °C. Work is ongoing to build a cell that can be safely used at much higher pressures. The use of zeolites as cement additives for obtaining tobermorite has been demonstrated previously [17]; they provide a reactive source of silica and alumina due to their large available surface areas [18], and they have been used as a starting material for tobermorite synthesis [19]. When silica is the additive, its physical characteristics are known to be important. For example, a lime-colloidal silica mixture (C/S=0.8) gave only C–S–H gel even after 20 h at 180 °C, whereas a similar mixture using quartz rather than colloidal silica produced well-crystallized tobermorite

after only 5 h [20]. In another study, colloidal silica gave only poorly crystalline tobermorite after 8 h at 180 °C [21].

## 2. Experimental

### 2.1. *In-situ* diffraction experiments

A sample cell employing sapphire tubing as the container for the hydrating cement slurry was used for high pressure and high temperature *in-situ* powder X-ray diffraction measurements. The cell [22] was developed in house. Pressure is applied to a column of cement slurry, ~1.6 mm diameter and several centimeters long, inside a sapphire tube, using oil pumped in from one end of the tube. The tube is surrounded by an aluminum heater block with apertures for the incident and diffracted X-ray beams. The pressure in the cement slurry is initially hydrostatic.

Using 3.2 mm o.d., 1.6 mm i.d. (1/8" o.d., 1/16" i.d.) sapphire tubes without the cement loaded gives an X-ray transmission of ~30% at 20 keV and ~60% at 30 keV, facilitating use at a reasonable range of synchrotron beam lines. Measurements were carried out at beam line 5BMD of the Advanced Photon Source, Argonne National Laboratory, using a 40 keV, 0.5 × 0.5 mm cross section, X-ray beam and a Mar345 image plate detector. Individual diffraction images were recorded every 288 s (exposure time 180 s, readout time 108 s). The 2D image files were converted to  $I/2\theta$  form using FIT2D [23]. Example integrated data are presented in Fig. 1 to illustrate their quality. The areas of characteristic Bragg peaks were determined, by curve fitting, as a function of time so that the time evolution of the relative amounts of the various crystalline phases in the sample could be followed. As synchrotron X-ray beam time is only available in limited amounts, each experimental run was terminated at the point where little additional information was likely to be obtained. Consequently, runs varied between about 4 and 12 h in duration depending upon the slurry composition and pressure under study.

The slurry compositions that were studied are listed in Table 1. The silica flour-containing slurry had a silica content known in practice to prevent strength retrogression [1,24]. The other slurry compositions were chosen to see how different sources of added silica influence the short term hydration chemistry, and potentially strength retrogression, when compared to that seen for the silica

Table 1  
Cement slurry compositions examined by *in-situ* diffraction methods

Slurry <sup>a</sup>	Class H cement (g)	Water (g)	Silica flour (g)	Zeolite (g)	Silica fume (g)	Cellulose derivative (g)	AMPS retarder (g)	Tartaric acid (g)
1 (C)	200	78.8	–	–	–	–	–	–
2 (SF)	100	135	35	–	–	1	–	–
3 (Z)	100	135	–	35	–	–	–	–
4 (ZS)	70	135	35	35	–	0.5	–	–
5 (AS)	100	135	–	–	35	1	–	–
6 (SFR)	200	82	70	–	–	–	1	1

<sup>a</sup> C control; SF cement+silica flour; Z cement+zeolite; ZS cement+zeolite+silica flour; AS cement+amorphous silica, SFR cement+silica flour+retarders.

flour. Each slurry was mixed at high speed in a Waring blender for 35 s, in accordance with API Recommended Practice 10B [25]. The delay between the initial mixing and the start of data collection was  $\sim 5$  min. After each slurry was loaded into the sample cell and pressurized, the temperature was ramped to 180 °C in 60 min.

## 2.2. Ultrasound transit time measurements

Each of the slurry compositions examined by *in-situ* diffraction methods was also independently examined using ultrasound. Ultrasonic techniques have been previously used to examine the evolution of mechanical properties with time as slurries hydrate, see for example the work of Boumiz and co-workers [26]. In the current paper, only transit times for compressional waves were measured. It has been established that these transit times (sound velocities) correlate with strength development after set has occurred [26,27].

The slurries were prepared according to API Recommended Practices 10B [25]. Transit times were measured on a Halliburton Ultrasonic Cement Analyzer with Chandler modifications for data acquisition. Samples were ramped to final temperature over 60 min. A pressure of  $\sim 10$  MPa (1500 psig) was applied, using water, at the beginning of each test. The pressure is initially hydrostatic. The transit time data are shown in Fig. 2.

## 2.3. Cement and additive specifications

An analysis of the Class H cement is given in Table 2. The silica flour used in preparing some of the slurries had a log mean diameter of  $\sim 17$   $\mu\text{m}$  and was  $\sim 99\%$  silica (quartz) by weight with some aluminum present ( $\sim 0.75\%$  by weight  $\text{Al}_2\text{O}_3$ ). The silica fume was an industrial byproduct and chemical analysis indicated that it was approximately 74% silica, 16% MgO and 3%  $\text{Fe}_2\text{O}_3$  by weight, with small amounts of various other metals present. The silica fume

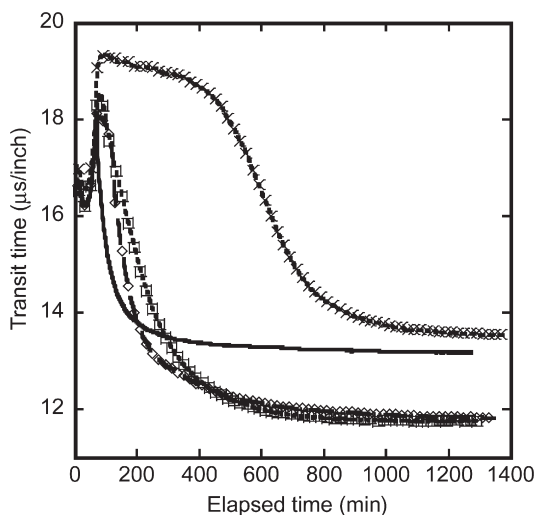


Fig. 2. Evolution of transit times for ultrasonic compression waves propagating through hydrating cement slurries. Crosses – slurry containing silica fume, solid line – slurry containing zeolite, squares – slurry containing silica flour, diamonds – slurry containing both zeolite and silica flour. Setting of the slurry containing silica fume is delayed relative to the other slurries.

Table 2  
Class H cement analyses

Oxide	%	Loss Corr.	Clinker	%
$\text{Na}_2\text{O}$	0.09	0.09	$\text{C}_3\text{S}$	47.13
$\text{MgO}$	1.08	1.09	$\text{C}_2\text{S}$	28.27
$\text{Al}_2\text{O}_3$	3.76	3.81	$\text{C}_4\text{AF}$	17.00
$\text{SiO}_2$	21.97	22.26	$\text{C}_3\text{A}$	0.65
$\text{SO}_3$	2.74	2.78	$\text{CaSO}_4$	4.72
$\text{K}_2\text{O}$	0.44	0.45	$\text{Na}_2\text{O}$	0.09
$\text{CaO}$	62.76	63.60	$\text{MgO}$	1.09
$\text{TiO}_2$	0.18	0.18	$\text{K}_2\text{O}$	0.45
$\text{MnO}$	0.07	0.07	$\text{TiO}_2$	0.18
$\text{Fe}_2\text{O}_3$	5.51	5.59	$\text{MnO}$	0.07
$\text{ZnO}$	0.01	0.01	$\text{ZnO}$	0.01
$\text{SrO}$	0.07	0.07	$\text{SrO}$	0.07
LOI	1.31	–	Free Lime	0.26

The phase composition is derived from a Bogue calculation, not direct analysis.

is expected to have a particle size of  $< 0.7$   $\mu\text{m}$ . Quantitative powder X-ray diffraction, using added silicon as a standard, indicated the presence of crystalline fersilicite ( $\text{FeSi} \sim 2.4\%$  by weight), periclase ( $\text{MgO} \sim 1.1\%$  by weight) and moissanite ( $\text{SiC} \sim 1.5\%$  by weight) as trace crystalline components of this additive. While this silica fume batch contains a high level of magnesium, this was not why it was chosen for use in the current study. The silica fume lies within the composition range that might be employed in the field. The ‘zeolite’ used in the present work was a naturally occurring mixture mined in Arizona. It was found, by laboratory X-ray powder diffraction, to contain clinoptilolite, heulandite and erionite, along with the sulfate minerals gypsum and bassanite. The silicon to aluminum ratio was estimated to be  $\sim 3:1$  by XRF and the loss on ignition suggested a water content of  $\sim 18\%$ . The total soluble sulfate content was estimated to be  $\sim 5\%$ .

## 2.4. Ex-situ X-ray powder diffraction measurements

Samples of slurry 5 (see Table 1) were prepared and cured at 180 °C in 125 ml Parr Bombs for 6, 10 and 24 h respectively. Powder X-ray diffraction data for these materials were recorded using a Scintag X1 diffractometer equipped with a copper radiation source and a Peltier cooled solid state detector.

## 2.5. Scanning Electron Microscopy

SEM images were recorded from fresh fracture surfaces using a Philips XL 30 ESEM. Samples were glued to SEM mounts, grounded with colloidal carbon paint around the sides and sputter coated with gold.

## 3. Results and discussion

Bassanite present in the zeolite additive was fully converted to gypsum during the initial mixing with water. In all the samples studied by diffraction, gypsum was fully depleted within the first 30–40 min of the *in-situ* X-ray measurements, in part *via* conversion to bassanite (water loss). Ettringite and monosulfate appeared only transiently during the ramp to final temperature.

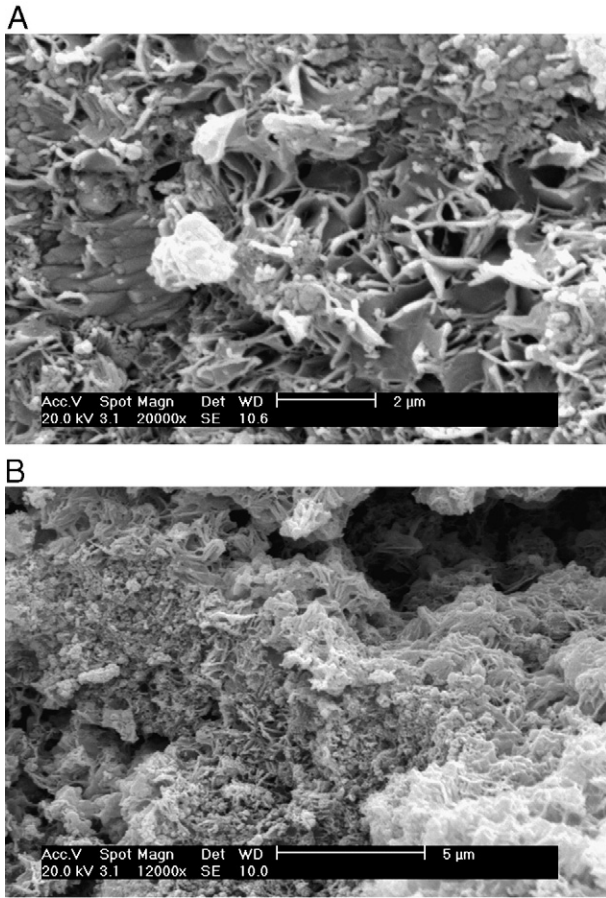


Fig. 3. SEM micrographs of samples containing silica fume that had been cured for A) 10 h and B) 4 h 20 min. The morphology seen for some of the hydration products may indicate the presence of tobermorite in the sample cured for 10 h.

Silica-substituted hydrogarnet (hydrogrossular) was seen in all slurries during the *in-situ* diffraction measurements; the cubic unit cell parameter,  $a$ , was close to 12.27 Å in all cases, indicating a composition close to  $C_3ASH_4$  [28]. However, the main crystalline hydration product, observed during the time period of our experiments, in all slurries, except those containing silica fume, was tobermorite. The final intensities of the tobermorite (002) peaks were more than 20 times greater than

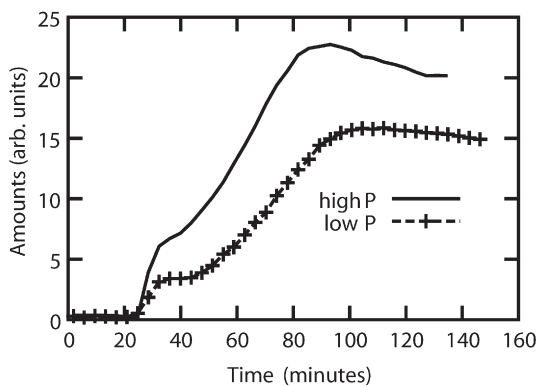


Fig. 4. Crystalline portlandite versus time in the control slurries (slurry 1 in Table 1). More portlandite is produced at 52 MPa than at 7 MPa.

those of the hydrogrossular (211) peaks. In the silica fume slurries, hydrogrossular was the only crystalline product observed. It is noteworthy that accelerated depletion of  $C_4AF$  was observed only in conjunction with tobermorite formation. No portlandite was seen for any slurry other than the control (no added silica), as expected.

The absence of any crystalline hydration products, other than the hydrogrossular, within the first 400 min for the slurry containing silica fume is consistent with our ultrasound transit data (see Fig. 2), as this slurry, unlike the others examined, does not develop significant compressive strength until >500 min. The role, if any, of the additive’s high MgO content in this is unclear. However, the *in-situ* X-ray data for the silica fume containing samples does not show any evidence of new magnesium-bearing phases, implying that the magnesium is incorporated into a typical crystalline cement hydration product or into the gel. A reduction in tobermorite formation when amorphous silica is used instead of crystalline silica is consistent with previous work [21,29]. SEM photographs of a silica fume containing sample, cured independently from the slurries used in the X-ray and ultrasound measurements, and recovered after 600 min at 180 °C show the presence of what may be microcrystalline tobermorite (Fig. 3A), with some morphological resemblance to published micrographs [19], but images of the same mix recovered from 180 °C after 260 min (Fig. 3B), do not show material of the same morphology, suggesting that the tobermorite forms after the 400 min examined by *in-situ* diffraction. *Ex-situ* powder diffraction measurements on samples cured for 6, 10 and 24 h only showed the presence of tobermorite at 24 h. The delayed development of compressive strength, observed only for the silica fume containing samples (see Fig. 2), seems to be associated with inhibition of  $C_3S$  hydration, as after the first 50 min of hydration out to the end of the diffraction measurements (~400 min) the  $C_3S$  does not appear to react at all. Inhibition of  $C_3S$  hydration has not been reported in previous studies examining the effect of amorphous silica addition on cement hydration.

The control slurries, with no additives and a w/c ratio of 0.394, gave mostly portlandite and jaffeite as crystalline products. An examination of portlandite production versus time at ~7 and 52 MPa (Fig. 4) shows a clear acceleration of portlandite on

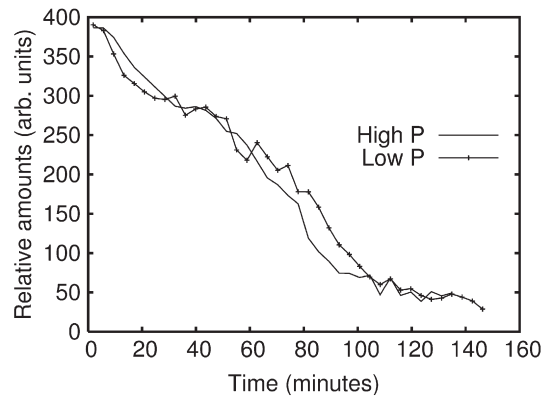


Fig. 5. Relative amount of  $C_3S$  versus time for slurry 1 (Class H control) at high and low pressure.

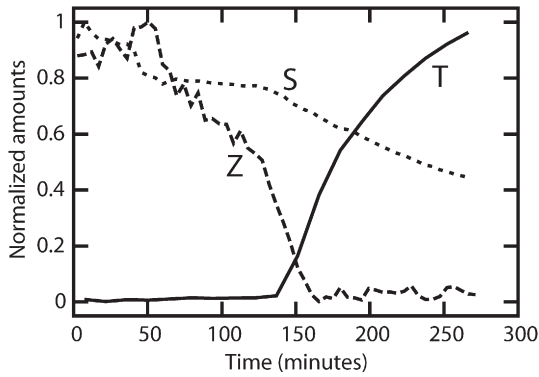


Fig. 6. Amount of silica flour (S), zeolite (Z) and tobermorite (T) versus time in slurry 4 hydrating at 7 MPa (low pressure). Both the silica flour and zeolite are reacting on the time scale of initial tobermorite formation. The Bragg scattering used to construct curve Z is primarily from heulandite with a contribution from an overlapping clinoptilolite peak.

increasing pressure at this temperature. This is qualitatively reflected in corresponding rates of  $C_3S$  depletion (Fig. 5); the slight loss of portlandite in the later stages can be attributed to reaction with the calcium silicates to form jaffeite.

In all the slurries containing silica flour and/or zeolite, tobermorite was by far the most abundant hydration product. Some  $\alpha-C_4AH_{13}$  appeared to form, but there was no evidence for the crystallization of hydrogarnet-type phases. Where both silica flour and zeolite are present, it is clear that both materials participate in the formation of tobermorite (Fig. 6). The tobermorite (002) peak position moves to lower angles in the sequence silica flour  $\rightarrow$  silica flour+zeolite  $\rightarrow$  zeolite, with  $d$  spacings 11.37, 11.47 and 11.55 Å respectively (Fig. 7). As the  $d$ -spacing of this peak is known to increase along with the aluminum content of the phase [11–13], the observed trend suggests an increase in aluminum substitution for tobermorite as the sequence silica flour  $\rightarrow$  silica flour+zeolite  $\rightarrow$  zeolite progresses. The rather oblate peak shape seen for the silica flour

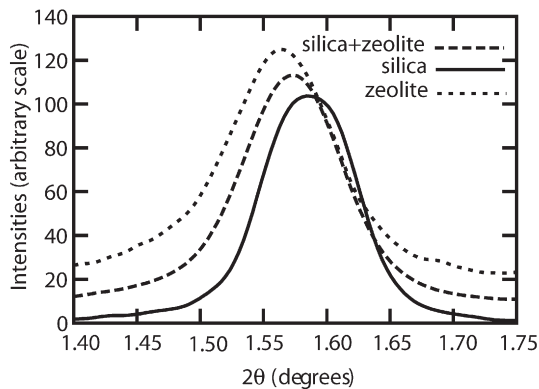


Fig. 7. The (002) peak of tobermorite systematically moves to lower angle as the added silica source is changed from silica flour, to a mixture of silica flour and zeolite, and finally to pure zeolite. This indicates that the extent of aluminum substitution in the tobermorite is increasing as we move to increasingly aluminum rich additives. The positions of this peak do not change significantly with time during the *in-situ* diffraction measurements.

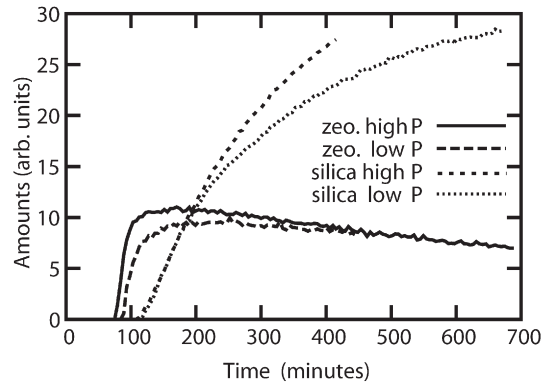


Fig. 8. Amount of tobermorite versus time for slurries containing just zeolite or just silica flour. Both the amount formed, and the onset of its crystallization, are largely independent of pressure.

sample suggests an aluminum distribution amongst the tobermorite crystals that might be bimodal, as two peaks with slightly different  $d$ -spacings from one another, due to differing aluminum contents, could give rise to the observed shape.

The intensity curves for tobermorite (002) crystallized from the silica flour and the zeolite samples show only slight acceleration due to increasing pressure (Fig. 8). The significance of the differences might be doubted, but since we have never observed retardation by pressure of silicate hydration reactions, it seems likely that the effect is real, but small. The effect of pressure is strong and beyond doubt, however, in the silica flour+zeolite slurries (Fig. 9). Not only does tobermorite form more rapidly, but the time for its onset is reduced by about a factor of 2. The measurements for this slurry were repeated at both high and low pressures, and the effect of pressure confirmed; the low pressure results are also in good agreement with those obtained previously under only autogenous pressure [30]. It is unclear why pressure should have such a pronounced effect on the hydration of this slurry, but no strong effect if only zeolite or silica flour is used. The accelerating effect of pressure on hydration kinetics has previously been reported for  $C_3S$  [15] and OPC [16], including the observation that the hydration of

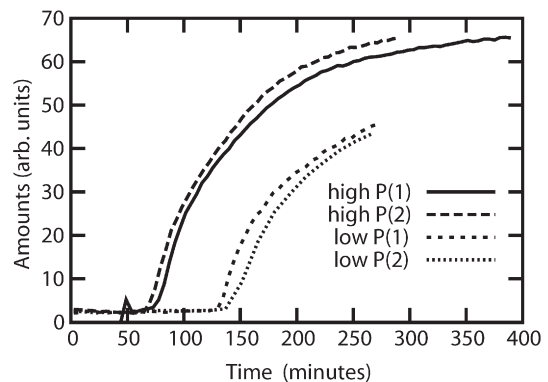


Fig. 9. Amount of tobermorite versus time for slurries containing a mixture of zeolite and silica flour. The time of initial crystallization is strongly dependent on pressure. Data for two runs at high and two runs at low pressure are shown to emphasize that this strong pressure effect is reproducible.

OPC was also increased as pressure was released. In the work on OPC, a gel membrane model for the pressure effect was proposed, but it is not clear how this could be extended to explain the composition dependence of the pressure effects that we see. The authors of the work on  $C_3S$  hydration explain their observed acceleration of hydration under pressure as a consequence of negative activation volumes. Once again, this general explanation for the effect of pressure is not easily extended to specifically explain the composition dependence of our observations. There is clearly a need for considerable further work on the role that pressure plays in the hydration of cements and cement phases, including the role of cement slurry composition.

Slurries containing silica flour and 0.5% bwoc tartaric acid + 0.5% bwoc sulfonated acrylamide copolymer retarders, showed qualitatively similar behavior to the silica-flour only mixes; but with the onset of tobermorite crystallization delayed until about 250 min after mixing. After its onset, tobermorite formation was again slightly more rapid under 52 MPa pressure.

#### 4. Summary

In all samples containing silica flour, zeolite, or both, the major crystalline hydration product was tobermorite. With silica fume as an additive, no major crystalline hydration products appeared within the  $\sim 400$  min of our *in-situ* measurements, but our other data suggests that tobermorite forms at longer times than this. Remarkably, the use of silica fume seems to inhibit  $C_3S$  hydration, not just the crystallization of calcium silicate hydrates. When only zeolite or only silica flour are used as mineral additives, pressure exerts very little influence on the crystallization of tobermorite, but there is a large pressure effect when both of these additives are present together.

#### Acknowledgements

This work was partly performed at the DuPont-Northwestern-Dow Collaborative Access Team (DND-CAT) Synchrotron Research Center located at Sector 5 of the Advanced Photon Source. DND-CAT is supported by the E.I. DuPont de Nemours & Co., The Dow Chemical Company, the U.S. National Science Foundation through Grant DMR-9304725 and the State of Illinois through the Department of Commerce and the Board of Higher Education Grant IBHE HECA NWU 96. We are very grateful for the assistance of DND-CAT staff while setting up the reported synchrotron experiments. Use of the Advanced Photon Source was supported by the U.S. Department of Energy, Basic Energy Sciences, Office of Energy Research under Contract No. W-31-102-Eng-38.

#### References

- [1] L.H. Eilers, R.L. Root, Long-term effects of high temperature on strength retrogression of cements, Society of Petroleum Engineers Paper 5028 (1974) 1–11.
- [2] K. Luke, Phase studies of pozzolanic stabilized calcium silicate hydrates at 180 °C, Cement and Concrete Research 34 (2004) 1725–1732.
- [3] G.L. Kalousek, A.F. Prebus, Crystal chemistry of hydrous calcium silicates: III, Morphology and other properties of tobermorite and related phases, Journal of the American Ceramic Society 41 (1958) 124–132.
- [4] S.O. Oyefesobi, D.M. Roy, Hydrothermal studies of Type V cement-quartz mixes, Cement and Concrete Research 6 (1976) 803–810.
- [5] J.J. Beaudoin, Calcium hydroxide in cement matrices: physico-mechanical and physico-chemical contributions, Materials Science of Concrete, Special Volume: Calcium Hydroxide in Concrete, 2001.
- [6] G.L. Kalousek, S.Y. Chaw, Research on cements for geothermal and deep oil wells, Journal of the Society of Petroleum Engineers 16 (1976) 307–309.
- [7] S. Shaw, C.M.B. Henderson, S.M. Clark, Hydrothermal formation of hydrated calcium silicates: an *in-situ* synchrotron study, American Mineralogist 62A (1998) 1337–1378.
- [8] G.L. Kalousek, Crystal chemistry of hydrous calcium silicates: I, Substitution of aluminum in lattice of tobermorite, Journal of the American Ceramic Society 40 (1957) 74–80.
- [9] P. Faucon, J.C. Petit, T. Charpentier, J.F. Jacquinet, F. Adenot, Silicon substitution for aluminum in calcium silicate hydrates, Journal of the American Ceramic Society 82 (1999) 1307–1312.
- [10] I.G. Richardson, A.R. Brough, R. Brydson, G.W. Groves, C.M. Dobson, Location of aluminum in substituted calcium silicate hydrate (C–S–H), Journal of the American Ceramic Society 76 (1993) 2285–2288.
- [11] M. Tsuji, S. Komarneni, P. Malla, Substituted tobermorites:  $^{27}Al$  and  $^{29}Si$  MASNMR, cation exchange, and water sorption studies, Journal of the American Ceramic Society 74 (1991) 274–279.
- [12] S. Diamond, J.L. White, W.L. Dolch, Effects of isomorphous substitution in hydrothermally-synthesized tobermorite, American Mineralogist 51 (1966) 388–401.
- [13] S.A.S. El-Hemaly, T. Mitsuda, H.F.W. Taylor, Synthesis of normal and anomalous tobermorites, Cement and Concrete Research 7 (1977) 429–438.
- [14] K.K. Ganguli, Studies on retardation of calcium silicate and calcium aluminate hydration at 150 °C 86.2 MPa, Ceramic Transactions 37 (1993) 21–35.
- [15] B. Bresson, F. Meducin, H. Zanni, Hydration of tricalcium silicate ( $C_3S$ ) at high temperature and high pressure, Journal of Materials Science 37 (2002) 5355–5365.
- [16] A. Rahman, A. D.D. Double, Dilatation of Portland cement grains during early hydration and the effect of applied hydrostatic pressure on hydration, Cement and Concrete Research 12 (1982) 33–38.
- [17] S. Komarneni, D.M. Roy, R. Roy, Al-substituted tobermorite: shows cation exchange, Cement and Concrete Research 12 (1982) 773–780.
- [18] T. Perraki, G. Kakali, F. Kontoleon, The effect of natural zeolites on the early hydration of Portland cement, Microporous and Mesoporous Materials 61 (2003) 205–212.
- [19] S. Komarneni, J. Komarneni, B. Newalkar, S. Stout, Microwave-hydrothermal synthesis of Al-substituted tobermorite from zeolites, Materials Research Bulletin 37 (2002) 1025–1032.
- [20] C.F. Chan, T. Mitsuda, Formation of 11 Å tobermorite from mixtures of lime and colloidal silica with quartz, Cement and Concrete Research 8 (1978) 135–138.
- [21] H. Sato, M. Grutzeck, Effect of starting materials on the synthesis of tobermorite, Materials Research Society Symposium Transactions 245 (1992) 235–240.
- [22] A.C. Jupe and A.P. Wilkinson, Sample cell for powder X-ray diffraction at up to 500 bar and 200 °C, Review of Scientific Instruments 77 (2006) 113901–113904.
- [23] A.P. Hammersley, S.O. Svensson, M. Hanfland, A.N. Fitch, D. Hausermann, Two-dimensional detector software: From real detector to idealised image or two-theta scan, High Pressure Research 14 (1996) 235–248.
- [24] G.W. Ostroot, W.W. Walker, Improved composition for cementing wells with extreme temperature, Journal of Petroleum Technology (1961) 277–284.
- [25] “Well simulation thickening time tests”; pp.18–21 in, Recommended Practice for Testing Well Cements, API Recommended Practice 10B. Ed. American Petroleum Institute, 1997.

- [26] A. Boumiz, C. Vernet, F. Cohen Tenoudi, Mechanical properties of cement pastes and mortars at early ages, *Advanced Cement Based Materials* 3 (1996) 94–106.
- [27] P.P. Rao, D.L. Sutton, J.D. Childs, W.C. Cunningham, An ultrasonic device for nondestructive testing of oilwell cements at elevated temperatures and pressures, *Journal of Petroleum Technology* (1982) 2611–2616.
- [28] R. Siauciunas, A. Baltusnikas, Influence of SiO<sub>2</sub> modification on hydrogarnets formation during hydrothermal synthesis, *Cement and Concrete Research* 33 (2003) 1789–1793.
- [29] J.L. LaRosa, S. Kwan, M.W. Grutzeck, Factors influencing the crystallization of tobermorite from C–S–H gel, *Ceramic Transactions* 37 (1993) 1–10.
- [30] A.C. Jupe, A.P. Wilkinson, K. Luke and G.P. Funkhouser, (unpublished results).